

Behaviour of Multi-Terminal Grid Topologies in Renewable Energy Systems Under Multiple Loads

Stavros Lazarou^{*1}, Catalin-Felix Covrig¹, Ilhami Colak^{1,2}, Philip Minnebo¹, Heinz Wilkening¹, Gianluca Fulli¹
stavros.lazarou@ec.europa.eu; Catalin-Felix.COVRI@ec.europa.eu; Aymen-CHAOUACHI@EC.EUROPA.EU; ilhami.colak@ec.europa.eu;
Philip.minnebo@ec.europa.eu; Heinz.Wilkening@jrc.nl; Gianluca.Fulli@ec.europa

¹ European Commission, Joint Research Centre, Institute for Energy and Transport, P.O. Box 2, 1755 ZG Petten - The Netherlands

² Gazi University, Faculty of Technology, Department of Electrical and Electronics Engineering, Ankara-Turkey

*Corresponding author: stavros.lazarou@ec.europa.eu, +31 224 565096

Abstract - Decarbonisation policies adopted worldwide are leading to an increasing deployment of renewable energy sources. In Europe, the growing number of offshore wind farm projects calls for scrutinising merits and opportunities of their interconnection via multi-terminal links rather than conventional point-to-point connections. The semiconductor components used in the converters and the resistance of power cables are expected to introduce new power losses in the transmission system. In this study, star and ring configurations with four DC nodes of multi-terminal grid topologies for renewable energy integration are modelled by means of NEPLAN software. In order to address more interconnection options the authors examine several grid topologies having more than three interconnections. The simulation results of the different network configurations, the power losses level in particular, are compared and analysed. The simulations illustrate an increasing complexity of network operation and power balancing, from a low power up to the rated power capacity injected at the inverters terminals.

Keywords: multi-terminal grid topology; modelling; real-time simulation; renewable energy; HVDC; smart grid.

I. INTRODUCTION

The contribution of renewable energy sources (RES) is of paramount importance to increase sustainability and security of energy supply. In the EU, among several renewable energy resources the offshore wind energy is currently considered as one of the most promising options. In fact, offshore wind farm installed capacity in Europe would reach 40GW by 2020 [1]. With increasing generation capacity and distance to shore of the wind farms, High Voltage DC (HVDC) transmission has been considered as more feasible option compared to conventional High Voltage AC (HVAC).

Beside the economical advantages, HVDC technology is providing benchmark solutions for the integration of remote renewable energy sources offering better operating flexibility and easier overload control. Recent technological progress and increasing needs for setting better electricity market opportunities resulted in the proposal of HVDC networks referred as Multi-Terminal HVDC grids. Compared to an HVDC point-to-point connection, MTDC can better support energy trading as well as a more efficient usage of the grid.

In fact, with respect to AC grids the MTDC can offer solutions to the following existing technological issues that still require further research:

- remote offshore generation connection;
- undersea or long distance interconnection;
- asynchronous grids coupling;
- reinforcement of feed-in into weak grids;
- grid reinforcement (e.g. pan-European overlay grid);
- isolated loads (e.g. offshore rigs, islands) connection.

Multi-terminal grids were proposed for the first time in 1963 [2]. J. Reeve published a review of available literature in 1980 [3]. Currently available technology offers two main schemes to develop HV MTDC grids:

- the Line-Commutated Converter (LCC-HVDC), which is based on the use of thyristors with constant DC current while the DC voltage is controlled to alter the power flow;

- the Voltage-Source Converter (VSC-HVDC), which is based on the use of force commutated switches, such as Insulated Gate Bipolar Transistors (IGBT). VSC-HVDC delivers a constant DC voltage while the current is controlled to alter the power flow allowing the use of cheaper cables.

The use of LCC-HVDC may be technically challenging to connect offshore wind farms [4]. On the other hand the VSC HVDC ability of creating independent AC voltage waveform allows the connection to weak islanded grids, including offshore wind farms.

For the wind park connections there is a tendency to consider VSC-HVDC technology [5], which offers some specific advantages [6]:

- VSC-HVDC can offer ancillary services by providing reactive power;
- VSC-HVDC does not increase the short circuit current of the AC system;
- the VSC-HVDC filter capacity is much lower compared to other solutions because of the sinusoidal Pulse Width Modulation (PWM) or multi-level topologies;

- given a fixed DC voltage polarity, VSCs can be interconnected thus forming a Multi-Terminal HVDC topology that can be defined as a DC network.

Recently researchers have been focusing on the optimisation of power flows in Multi-Terminal HVDC grids in order to reduce the total power loss of the system [7-12]. Negra et al. [7] compare the transmission losses for different HVDC and HVAC systems. Their results concluded that HVAC system achieved the lowest losses for distances up to 55-70 km from the shore whereas the LCC-HVDC technology had lower losses than the VSC-HVDC solution for the same distance range. Montilla-Djesus et al. [8] studied the optimal operation of an offshore wind farm, consisting of 120 wind turbines connected to the grid using HVDC.

In order to achieve optimal operation of the wind park, the distribution of the reactive power set points throughout the wind turbine generators must be optimal, leading to minimum losses within the wind farm and the HVDC transmission system. Haileselassie and Uhlen [9] investigated power flow in Multi-Terminal HVDC networks involving a method based on the Newton-Raphson approximation. Veilleux and Ooi [10] studied two configurations: a 3 terminals system / 3 lines and a 4 terminals system / 5 lines. Da Silva and Castro [11] investigated the influence on voltage regulation of the onshore connection bus in a multi-bus test power system. The simulation results show that (compared to a HVDC system) the HVAC solution is limited by the distance to shore and by the wind transmitted power. Da Silva et al. [12] analyze a Multi-Terminal Grid using an EMTDC-PSCAD platform.

In this study, power losses of representative Multi-Terminal Grid Topologies for RES integration are identified and analysed using NEPLAN simulation models. The simulations illustrate an increasing complexity of network operation and power balancing from a low power level up to the rated power capacity injected at the inverters terminals. In order to generalize the obtained results regarding to the all possible connection options, topologies having more than three points are considered. Power losses of the network configurations under study are compared and analyzed.

II. MULTI-TERMINAL GRID TOPOLOGIES UNDER STUDY

This study has been carried out using NEPLAN software [13]. Power flow optimisation is carried out via the Extended Newton-Raphson method, which provides adequately low simulation time. The maximum number of iterations was set to 40 and the convergence mismatch to 10^{-8} .

The schematic models given in Fig. 1 and Fig. 2 are composed of separated elements. Four network feeders, four node busses, four converter elements and a number of DC-lines were used for each model. The network feeders have a short circuit level $Sk_{max} = 25010.8$ MVA, a short circuit current

$Ik_{max} = 38$ kA, $R(1)/X(1) = 0.1$ pu, $Z(0)/Z(1) = 3.029$ pu and $R(0)/X(0) = 0.15$ pu. The operational voltage level is 1 pu in all the connection nodes. The converter elements operate as inverters or rectifiers. The rectifiers in these models inject a given amount of power into the system or they keep the voltage on the DC side stable (slack nodes). The converter EL2 as

given in Figs. 1 and 2 is the system slack and keeps the voltage at its secondary side on the level of 666.75 kV. Its internal resistance was set to $X_c = 4.8106 \Omega$. The converter EL21 as depicted in Figs. 1 and 2 is a rectifier operating as an injector of a given power to the system. This power changes according to the parametric analysis presented in the next chapter. Its internal resistance was set to $X_c = 6.848 \Omega$.

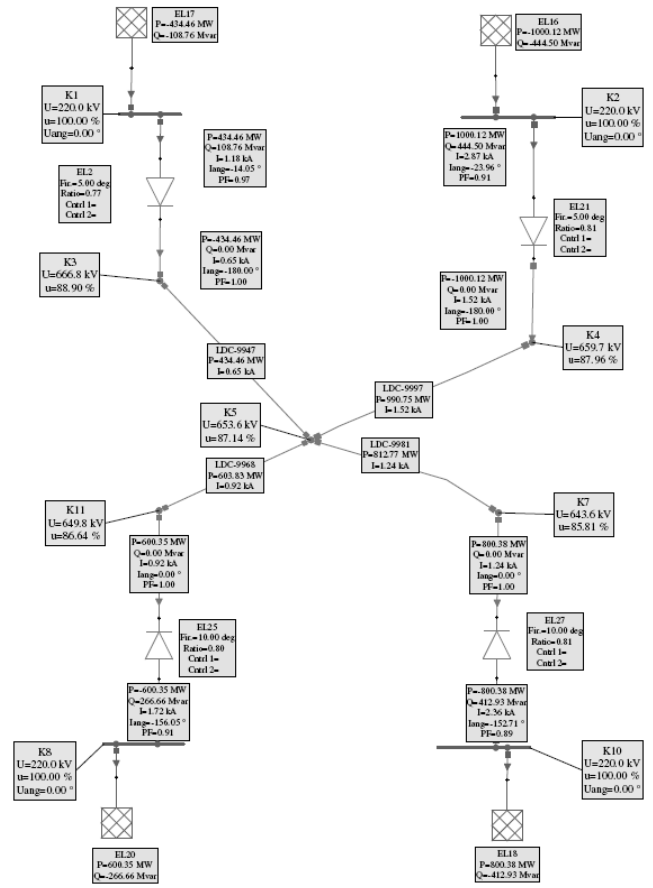


Fig. 1 Schematic NEPLAN model including four DC nodes connected in star configuration

The converter EL25 operates as inverter feeding EL20 as illustrated in Figs. 1 and 2. Its internal resistance was set to $X_c = 9.523 \Omega$. The converter EL27 operates as inverter feeding EL18 as shown in Figs. 1 and 2. Its internal resistance was set to 9.7683Ω . The DC lines have a resistance value of $4.078 \Omega/\text{km}$.

In the star topology of Fig. 1 all nodes are individually connected to a central hub. Failure of this hub will cause the entire network to shut down. In the ring configuration of Fig. 2 one cable sequentially connects all nodes, forming a closed loop. In this case the transferred energy should by-pass the adjacent nodes increasing energy losses. This study focuses on a four nodes system for both topologies, where all possible

network topologies can be practically reduced to the studied configurations.

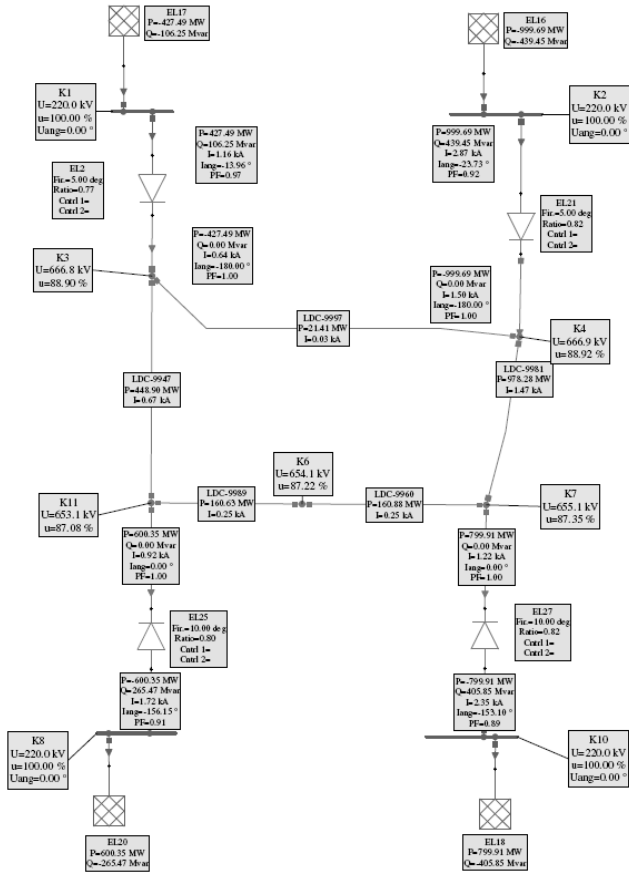


Fig. 2 Schematic NEPLAN model including four DC nodes connected in ring configuration

II. RESULTS AND DISCUSSION

For the sake of simplification all the networks illustrated in Fig.1 and Fig. 2 were modified as following: Node 1 (N1) represents the slack node of the system. Node 2 (N2) represents the generation node where Nodes 3 and 4 (N3, N4) represent the loads connected to feeders. Practically in MVDC network N1 and N2 are the connection points of RES (e.g. offshore wind farms) whereas N3 and N4 could represent the connection points with the AC grids. They should be flexible enough to absorb the energy produced.

The star configuration includes the node 5 (N5) which is the common network node. The DC lines of the system are named using the acronyms LDC 1 to 4 as depicted in Figs. 3 and 4.

The simulation scenarios consisted on a variable injection of the power generated by the RES production which results in power flow and network total power losses variations.

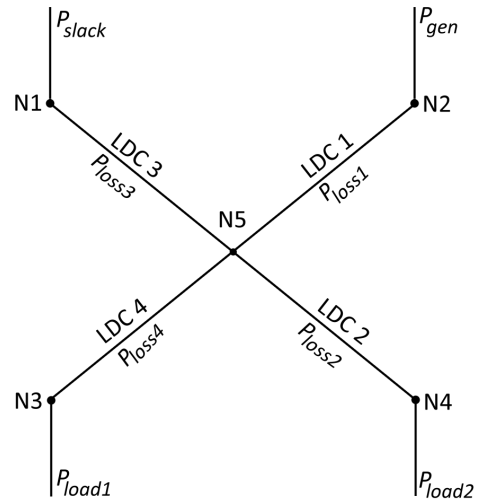


Fig. 3. Single line representation of the four DC nodes connected in star configuration

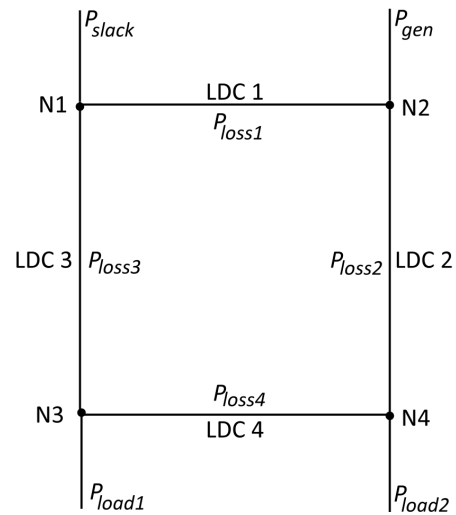


Fig. 4. Single line representation of the four DC nodes connected in ring configuration

The analysis was performed by injecting the active power P_{gen} varies from 100 MW to 1300 MW at node N2, for both the star and the ring configurations, as depicted in Fig. 5 and 6. When the injected power at node N2 in the star topology is 100MW, the losses in line LDC1 are around 1MW and negligible, while the losses in line LDC3 are higher reaching 33MW, since the line associated to the slack node N1 is more stressed in order to reach the system load balance keeping the same load demand at the nodes N3 and N4.

IV CONCLUSIONS

It was observed that there is a local minimum for the power losses, irrespectively of the topology (star or ring) used for multi-terminal HVDC grids. Consequently, in order to optimise the performance of a system, it is proposed to perform the parametric analysis described in this paper and to identify the losses local minimum. This local minimum can be moved according to the project needs by modifying the type and the resistance of the DC cables installed.

The simulation results will be validated and expanded in the future with hardware-in-the-loop experiments in the Smart Grid Simulation Centre of the European Commission's Institute for Energy and Transport (IET). In particular, additional studies are needed to assess performances of a global power system embedding one or more multi-terminal HVDC grids.

ACKNOWLEDGMENT

The authors would like to thank Panagiotis Kontodimos and Rossano Musca from BCP for their contribution.

REFERENCES

- [1] "Pure Power: Wind energy targets for 2020 and 2030," European Wind, Energy Association, Tech. Rep., 2009.
- [2] U. Lamm, E. Uhlmann, P. Danfors, Some aspects of tapping HVDC transmission systems, *Direct Current* 8 (5) (1963) 124–129
- [3] J. Reeve, Multiterminal HVDC power systems, *IEEE Transactions on Power Apparatus and Systems* PAS 99 (2) (1980) 729–737
- [4] D. Hertem, M. Ghandhari, "Multi-terminal VSC HVDC for the European supergrid: Obstacles," *IEEE Transactions on Power Delivery*, vol.14, no.9, pp. 3156-3163, Mar.2010.
- [5] J.Yang, J.E. Fletcher, J.Reilly"Multiterminal DC Wind Farm Collection Grid Internal Fault Analysis and Protection Design"IEEE Transaction on Power Delivevery,Vol,25,No,4,2010.
- [6] G. Li, G.Li, L. Haifeng, Y. Ming, "Research on Hybrid HVDC"International Conference on Power System Technology, PowerCon, 2004.
- [7] Negra, N.B., Todorovic, J., Ackermann, T., "Loss evaluation of HVAC and HVDC transmission solutions for large offshore wind farms", *Electric Power Systems Research* 76 (2006) 916–927
- [8] Montilla-Djesus, M., Santos-Martin, D., Arnaltes, S., Castronuovo, E.D. "Optimal reactive power allocation in an offshore wind farms with LCC-HVdc link connection", (2012) *Renewable Energy*, 40 (1), pp. 157-166
- [9] Haileselassie, T.M., Uhlen, K., "Power flow analysis of multi-terminal HVDC networks", 2011 IEEE PES Trondheim PowerTech: The Power of Technology for a Sustainable Society, POWERTECH 2011
- [10] Veilleux, E., Ooi, B.-T. "Power flow analysis in multi-terminal HVDC grid", (2011) 2011 IEEE/PES Power Systems Conference and Exposition, PSCE 2011,
- [11] Da Silva, F.F., Castro, R., "Power flow analysis of hvac and hvdc transmission systems for offshore wind parks", (2009) *International Journal of Emerging Electric Power Systems*, 10 (3).
- [12] Da Silva, R., Teodorescu, R., Rodriguez, P., "Power delivery in multiterminal VSC-HVDC transmission system for offshore wind power applications", *IEEE PES Innovative Smart Grid Technologies Conference Europe, ISGT Europe*
- [13] NEPLAN software website, <http://www.neplan.ch>

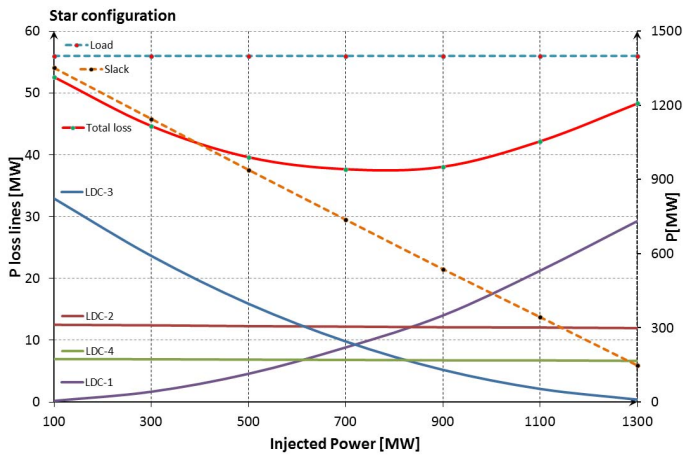


Fig. 5. Power losses in the star configuration

When injected power at node N2 in the star topology is increased from 100 MW to 300 MW, the losses in LDC1 are increased from 0 to 2 MW while the losses in LDC3 are decreasing from 33 MW to 24 MW, so that the total losses of the system are decreased. If the injected power at node N2 is 500 MW, the decrease of the total power loss is more important and the losses on LDC3 and in LDC1 are reduced to 15 MW and 5 MW respectively. For the star configuration, the minimum total loss occurs when 730 MW of power is injected at node N2.

In the ring topology for 100 MW of injected power, line LDC3 has a maximum loss of 13 MW while line LDC2 presents its minimum losses of 6 MW. In this case the total losses are 24 MW. If the injected power at node N2 is 300 MW, the total losses decrease to 22 MW while the optimal power injection level is equal to 730 MW corresponding to a total power loss of 18 MW.

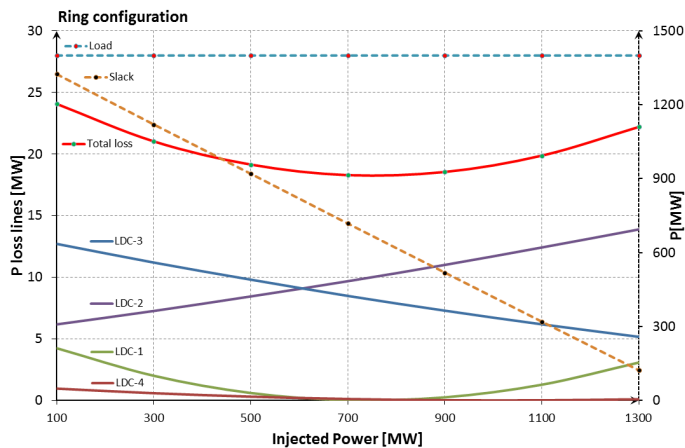


Fig. 6. Power losses in the ring configuration

It has to be mentioned that the model developed can be used effectively on short circuit simulations. The information needed for short circuit simulations has been included in all the applicable modules of the model.